Arabian Journal of Chemistry (2021) **14**, 103238

King Saud University

Arabian Journal of Chemistry

www.ksu.edu.sa
www.sciencedirect.com

ORIGINAL ARTICLE

Amelioration of oxidative stress, inflammation and tumor promotion by Tin oxide-Sodium alginate-Polyethylene glycol-Allyl isothiocyanate nanocomposites on the 1,2-Dimethylhydrazine induced colon carcinogenesis in rats

Wei Wei [a], Rongxian Li [a], Qinghang Liu [a], Vidya Devanathadesikan Seshadri [b], Vishnu Priya Veeraraghavan [c], Krishna Mohan Surapaneni [d], Thamaraiselvan Rengarajan [e,*]

[a] *Department of Anorectal, Xinxiang Central Hospital, The Fourth Clinical College of Xinxiang Medical University, Xinxiang City, Henan Province 453000, China*
[b] *Department of Pharmacology & Toxicology, College of Pharmacy, Prince Sattam Bin Abdul Aziz University, Al-Kharj, Saudi Arabia*
[c] *Department of Biochemistry, Saveetha Dental College, Saveetha Institute of Medical and Technical Sciences, Saveetha University, Chennai 600 077, India*
[d] *Department of Biochemistry, Panimalar Medical College Hospital & Research Institute, Varadharajapuram, Poonamallee, Chennai 600 123, India*
[e] *Scigen Research and Innovation Pvt. Ltd., Periyar Technology Business Incubator, Thanjavur, Tamil Nadu, India*

Received 2 April 2021; accepted 27 May 2021
Available online 3 June 2021

KEYWORDS

Colon cancer;
Oxidative stress;
Inflammation;
Allyl isothiocyanate;
1,2-Dimethyl hydrazine

Abstract *Background:* Colorectal cancer (CRC) is a frequently diagnosed cancer that primarily affects the digestive system and an imperative cause of mortalities worldwide.

Objective: In this work, we formulated the Tin oxide-Sodium alginate-Polyethylene glycol-Allyl isothiocyanate nanocomposites (SAP-Ally-NCs) and investigated its anticancer role against the DMH-provoked CRC in rats.

Methodology: The formulated SAP-Ally-NCs were characterized different techniques. The CRC was provoked to the rats via injecting 20 mg/kg of DMH and then administered with the formulated

* Corresponding author.
E-mail address: thamarairaj2000@gmail.com (T. Rengarajan).
Peer review under responsibility of King Saud University.

Production and hosting by Elsevier

https://doi.org/10.1016/j.arabjc.2021.103238

SAP-Ally-NCs for 16 weeks. The bodyweight changes and the polyp's incidences were detected and tabulated. The status of lipid peroxidation and antioxidant enzymes were studied by standard techniques. The inflammatory markers and xenobiotic enzymes level was scrutinized using respective kits. The mRNA expressions of various signaling molecules were examined by RT-PCR. The liver and colon tissues were examined microscopically to detect the histological changes.

Results: The formulated SAP-Ally-NCs treatment appreciably improved the body weight gain and suppressed the polyp's incidences in the DMH-challenged animals. SAP-Ally-NCs treated animals were demonstrated the notable reduction in the lipid peroxidation and inflammatory cytokines and elevated the antioxidant enzymes i.e. CAT and SOD activity. SAP-Ally-NCs administered animals exhibited the noticeable reduction in the expression of PCNA, cyclin-D1, iNOS, and COX-2 in the colon tissues. The histological findings also unveiled the therapeutic role of SAP-Ally-NCs.

Conclusion: In conclusion, the SAP-Ally-NCs demonstrated the potent anticancer action against the DMH-provoked CRC in rats. In future, it could be a potent chemotherapeutic agent to the CRC.

1. Introduction

The colorectal cancer (CRC) is the third most often identified worldwide among the deadliest non-communicable diseases and ranked second in terms of death rate globally (Bray et al., 2018). CRC is a multifaceted ailment with elevated incidences in Western countries as well as Asian countries. This ailment is closely related with alterations in the dietary patterns like over utilization of ultra-processed commercial foods and beverages with poor nutritional rate (Poti et al., 2017). Oxidative stress affects normal cellular functions via triggering DNA injury, lipid peroxidation, and mutations. Furthermore, the tight connection between oxidative markers and CRC progression was unveiled by numerous findings (Mariani et al., 2014; Rashid, 2017; Ahmed et al., 2019). The cellular injury due to the inequity between ROS accumulation and antioxidants status could result in DNA damage and mutations (Liu et al., 2017). Another event participating in the CRC progression is the continual local inflammatory responses due to the augmented generation of the pro-inflammatory regulators like IL-6, IL-17, and tumor necrosis factor (TNF-α) in an struggling to reinforce the damaged cells (Tuomisto et al., 2019; De Almeida et al., 2018).

The antioxidant systems play an immense role in order to neutralize the ROS and declining its cellular damage. This is a most complicated system that contains both enzymatic and non-enzymatic antioxidants (Birben et al., 2012). Antioxidants performs a crucial function in the direct hunting of ROS or indirectly interfaces ROS accumulation and thereby terminating its toxic effects (Pisoschi and Pop, 2015). Recently, targeting the antioxidant systems are regarded as a most promising strategy to counteract the numerous ailments especially CRC, as they minimizing the acquisitive harmful effects of oxidative injury (Schieber and Chandel, 2014; Sosa et al., 2013). The upsetting incidences of CRC were led to an unrelenting need for exploring novel therapies that could overawed the restrictions of existing therapies. Based on the stage of cancers, therapeutic procedures often include surgery, radiation and chemotherapy. CRC is normally detected in a late stages, when victims regularly diagnosed with reserved metastases (Van der Stok et al., 2017; Van Cutsem et al., 2016; Hammond et al., 2016; Braun and Seymour, 2011).

Inflammation is a normal biological event that takes place during the infection/damage. It triggers the immune system to discharge pro-inflammatory mediators in order to guard our body. Nonetheless, excessive inflammatory reactions are extremely dangerous. There are tight connections between inflammation and cancers as it is one of the prime event of cancer. Inflammatory reactions aggravate the tumor progression through avoiding the cellular differentiation and endorsing tumor development (Klampfer, 2011). The over-production of inducible nitric oxide synthase (iNOS) could cause the DNA injury, DNA repair deficient, promotion of cancerous growth. (Senedese et al., 2019). The PCNA is a non-histamine nuclear protein, which contributes a major function in the DNA replication with the rebuilding of the DNA double strands, and is regarded as an indicator of proliferative index and cell cycle kinetics. PCNA status has straight connections with the malignancy, invasion, penetration, and survival of tumor cells (Cai et al., 2017; Guzinska-Ustymowicz et al., 2009).

A remarkable progress in chemotherapy for CRC treatment was made and it still demonstrating one of the keystones of anticancer therapy. Though, far from a perfection of chemotherapy, it is unavoidably connected with multidimensional challenges and dose-associated toxicities because of the off-target accretion and less pharmacokinetics that restricts its therapeutic potential and vulnerability to multi-drug resistance during treatments (Guimaraes et al., 2015). Currently, carrying safer and potential dosages of target drugs is a vital goal of contemporary chemotherapeutic approach and these dosages will target the sites of the disease and standby the normal cells (Gullotti and Yeo, 2009). Consequently, to address this problem a selective drug delivery system needs to be explored (Mohanty et al., 2020).

Nanodrug-delivery systems have received much attention as a potent drug delivery approach, accordingly demonstrating an advanced technique for well-ordered and targeted release of the drug to tumors as they may lessen the toxic outcomes and elevate the effectiveness of the anticancer treatment (Wu et al., 1853; Mukherjee et al., 1937). Sodium alginate (SA) is a most conventional, degradable, non-toxic, and well-matched biopolymer with an extensive utilizations (Tang et al., 2018; Zhou et al., 2019). In recent times, numerous findings has explored the nano-materials combined with SA in order to elevate the functional and technological features of SA-based nano-materials (Thakur and Arotiba, 2018; Naik et al., 2016). 1,2-Dimethyl hydrazine (DMH), is a strong colon carcinogen, provoking CRC in the investigational animals (Newell and Heddle, 2004; Saini et al., 2009) and it is a extensively executed model of chemically-provoked CRC. DMH-triggered CRC is a multifaceted mechanisms involving an array of pathological modifications (Ionov et al., 1993).

Allyl isothiocyanate is a strong, volatile, color-less oil that is found in *Brassica* plants of the Cruciferae family (Sharma et al., 2012). Allyl isothiocyanate is found to suppress the viability, multiplication, invasion, and to trigger the apoptotic cell deaths in the different human cancer cells like liver, cervical, and bladder (Zhang, 2010; Hwang and Lee, 2006; Qin et al., 2018; Savio et al., 2015). Furthermore, the effectiveness of Allyl isothiocyanate in combination with radiation therapy is most effective against the non-small cell lung cancer cells (Tripathi et al., 2015). In this exploration, we fabricated the Tin oxide-Sodium alginate-Polyethylene glycol-Allyl isothiocyanate nanocomposites (SAP-Ally-NCs) and evaluated its anticancer potential against the DMH-triggered CRC in rats through the minimizing of oxidative stress and inflammation.

2. Materials and methods

2.1. Chemicals

Allyl isothiocyanate, Tin oxide, Sodium alginate, Polyethylene glycol, and other chemicals were attained from the Sigma-Aldrich, USA. The assay kits for inflammatory markers were procured from eBioscience, CA, USA. The PCR kits were attained from the Thermofisher, USA, and Takara Bio, Japan, respectively.

2.2. Formulation of SAP-Ally-NCs

The preparation of SAP-Ally-NCs: 0.3 g of SnO_2 NPs was added to 20 mL of Sodium alginate solution, then SnO_2-Sodium alginate solution mixture was added into 20 mL of Polyethylene Glycol (PEG). Finally, the whole SnO_2-Sodium alginate-PEG homogenizes mixture solution was encapsulated with 50 μL of Allyl isothiocyanate solution. The SAP- Allyl nanocomposites were stirred continuously at 80 °C for 6 h. A white precipitate was formed on continuous stirring; the residue was centrifuged at 15,000 rpm for 15 min at −4 °C. The solid SAP-Ally precipitate was washed several times with deionized water. Finally, the SAP-Ally nanocomposites were dried at 200 °C for 3 h.

2.3. Characterization techniques

The formulated SAP-Ally-NCs were characterized by an X-ray diffractometer (X'PERT PRO PANalytical). The SAP-Ally-NCs was investigated through the Field Emission-Scanning Electron Microscopy (Carl Zeiss Ultra 55 FESEM) with EDAX (Inca). The formation of SAP-Ally-NCs was confirmed by UV–Visible spectroscopy (Perkin Elmer Instrument, USA). The active biomolecules of the formulated SAP-Ally-NCs were studied by Fourier transform infrared (FT-IR) analysis in the wavenumber 500–4000 cm^{-1}. Photoluminescence spectra analysis was done using the Cary Eclipse spectrometer.

2.4. Animals

The 4 to 6-week-aged male Wistar rats, weighing 120–150 g was collected from Institutional animal housing facility. Animals were then sustained beneath the usual laboratory situations with 45–55% humidity, 23–25 °C temperature and 12 h light/dark series. All animals having free contact to regular diet and water throughout the experimental tenancy. All animal experiments were verified and approved by the institutional animal ethical committee.

3. Experimental regimen

The 24 rats were arbitrarily alienated into four groups with 6 animals in each. Control (group I) animals were administered with regular standard diet without any treatments. Group II rats in were administered with 20 mg/kg of DMH (dissolved in 1 mM EDTA, pH-6.5) via subcutaneous route, once in a week for 5 successive weeks to initiate the CRC (Colussi et al., 2001). Animals from group III and IV supplemented with low and high dose of formulated SAP-Ally-NCs (10 and 15 μM), respectively concurrent with DMH challenge. The formulated SAP-Ally-NCs treatment was continued till the 16th week. At the end, bodyweight, weight gain, and growth rate were determined via applying the following formula:

$$\text{Weight gain} = \text{Bodyweight(final)} - \text{Bodyweight(initial)}.$$

$$\text{Growth rate} = (\text{Bodyweight(final)} - \text{Bodyweight(initial)})/\text{No. of experimental days.}$$

3.1. Measurement of polyp's incidence

The whole colon tissues were excised after the animal sacrification at the end of experiments. Then the excised colon tissues were cleansed with saline and incised longitudinally without interrupting the developed polyps and guardedly enumerated via macroscopic monitor.

3.2. Determination of lipid peroxidation and antioxidant enzymes activity

The liver, proximal and distal colon tissues of experimental animals were excised and the same was homogenated separately using buffered saline. The tissue homogenates were utilized for the biochemical assays. The status of lipid peroxidation was investigated through detecting the levels of thiobarbituric acid reactive substances (TBARS) by the method suggested by Ohkawa et al. (1979). The enzymatic activity of superoxide dismutase (SOD) was defined as the enzyme level resulting 50% of inhibition in pyrogallol autoxidation, which was executed as suggested by the Marklund (1985) and the outcomes were demonstrated as SOD min/mg protein. Catalase (CAT) activity was investigated via its capacity to breakdown hydrogen peroxides into the water and oxygen, which was scrutinized as per the protocols suggested by Aebi (1984) and the outcomes were depicted as CAT μM/min/mg protein.

3.3. Determination of phase I and phase II xenobiotic enzymes

Cytochrome P450 status was detected with the aid of Omura & Sato (1964) approach and Cytochrome 4502E1 was investigated by the protocols of Watt et al. (1997). The status of Cytochrome-b5, NADPH-Cytochrome P450 Reductase and NADPH-Cytochrome b5 Reductase was scrutinized as per the procedures of Gan et al. (2009).

3.4. Detection of inflammatory markers

The status of pro-inflammatory mediators like TNF-α, IL-6, and IL-1β in the serum of experimental animals was scrutinized with the help of respective assay kits (eBioscience, CA, USA). All assays were done as per the protocols given by the kit's manufacturer.

3.5. Histological analysis

The liver and colon tissues of experimental animals were excised and processed with saline. Paraffin embedded liver and colon tissues were then sliced at 5 μm and mounted on

clean glass slides. After the dewaxing and rehydration, a pair of slides was stained with hematoxylin and eosin (H&E). Lastly, the slides were monitored beneath the optical microscope to detect the histological alterations in the liver and colon tissues.

3.6. RT-PCR analysis

Total RNA extraction was done with the aid of TRIzol kit by applying instructions of manufacturer (Thermofisher, USA). RNA amount was determined using NanoDrop spectrophotometer. Then, the RNA was utilized to construct the cDNA with the help of kit with manufacturer's protocols. RT-PCR examination was executed to with the help of commercial kits (Takara Bio, Japan). The primers for PCNA sense: 5′-CCAT CCTCAAGAAGGTGTTGG-3′, antisense: 5′-GTGTCCCA TATCCGCAATTTTAT-3′, Cyclin-D1 sense: 5′-CCGTCCA TGCGGAAGATC-3′, antisense: 5′-GAAGACCTCCTCCT CGCACT-3′, iNOS sense: 5′-CACCACCCTCCTTGTT CAAC-3′, antisense: 5′-CAATCCACAACTCGCTCCAA-3′, and COX-2 sense: 5′-AGGAGATGGCTGCTGAGTTGG-3′, antisense: 5′-AATCTGACTTTCTGAGTTGCC-3′ were utilized. The 2–ΔΔCT approach was utilized to determine the relative expressions of target genes and normalized with the housekeeping gene β-actin expression.

3.7. Statistical analysis

The outcomes were depicted as the mean ± SD from all the discrete groups. The one-way ANOVA was applied to illustrate the variations between groups successively Tukey–Kramer's multiple comparison assay, and the statistical significance is set at $p < 0.05$ for all assessments.

4. Results

4.1. Characterization of formulated SAP-Ally-NCs

The XRD patterns of SAP-Ally-NCs are shown in Fig. 1. The XRD characteristic peaks at 2θ = 26.44° (1 1 0), 33.76° (1 0 1), 37.71° (2 0 0), 51.63° (2 1 1), 54.62° (2 2 0), 57.84° (0 0 2), 61.80° (3 1 0), 64.45° (1 1 2), 65.76° (3 0 1), 71.10° (2 0 2) and 78.54° (3 2 1) is corresponds to tetragonal structure of Tin oxide-Sodium alginate-Polyethylene glycol- Allyl isothiocyanate nanocomposites. The prepared nanocomposites results is good agreement with JCPDS no. 88-0287 and peaks show that the tetragonal rutile-type SnO_2 (space group P42/mnm) crystalline structure. The present results confirmed that Sodium alginate -Polyethylene glycol- Allyl isothiocyanate molecules have successfully substituted on the SnO_2 surface matrix. The average crystallite size is found to be 122 nm calculated using Debye-Scherrer formula (D) = $\frac{0.9\lambda}{\beta\cos\theta}$.

The SEM image of SCP-Ally nanocomposites that determine the size and morphology are shown in Fig. 2(a-b). The SCP-Ally nanocomposites are formed spherical with a stone like nanostructure and the average particle size is 126 nm. The chemical composition of SCP- Ally nanocomposites are identified by EDX spectra as shown in Fig. 2(c). From the

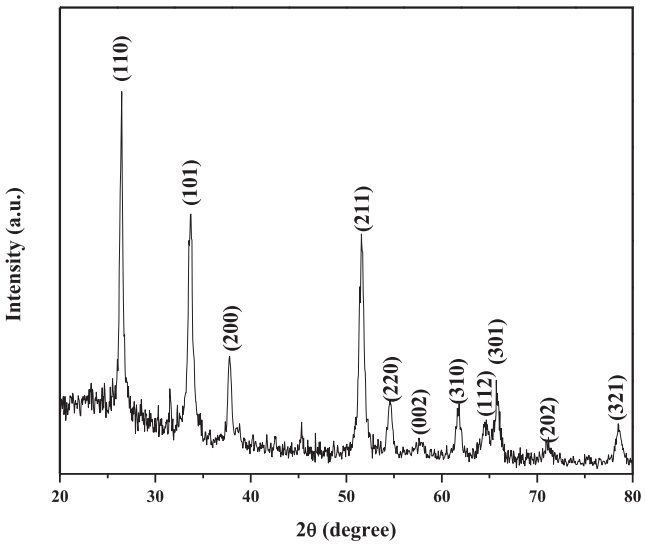

Fig. 1 X-ray diffraction pattern of SAP-Ally-NCs.

EDX results, the nitrogen, carbon, tin and oxygen molecules are clearly observed for SCP- Ally nanocomposites. The atomic percentages were, found to be: 7.37% of Sn and 58.29% of O, 32.54% of C, and 1.79% of N in the SCP- Ally nanocomposites.

An FTIR spectrum for SAP-Ally nanocomposite is shown in Fig. 3, which is reveals the presence of functional group such as –OH and Sn-O. The O-H stretching bands are around 3454 cm^{-1} and 1633 cm^{-1}, correspond to the absorption of water molecules at the sample surface. The asymmetric O-Sn-O stretching vibrations have occurred at 835 and 626 cm^{-1}, which has indicated that the SnO_2.

The UV–vis absorption spectrum of the SAP-Ally nanocomposites was shown in Fig. 4. The UV–vis absorption spectrum of the SAP-Ally nanocomposites synthesized at temperatures 200 °C. In the present work, the absorbance edge peak is observed at 282 nm for SAP-Ally nanocomposites.

The photoluminescence spectrum of the SAP-Ally nanocomposites, with an excitation wavelength of 325 nm is shown in Fig. 5. The emission spectrum of the SAP-Ally nanocomposites, the peaks at 367 nm, 403 nm, 435 nm, 476 nm, 505 nm and 538 nm respectively. The Near band edge (NBE) emission is found to be 367 nm, corresponding to the recombination of electron-hole pairs in oxygen and metal vacancies. The violet emission located at 403 nm, due to the recombination of the CB electron to the V_o^{2+}. The blue emission peaks are found to be 435 nm and 476 nm, is attributed to the electron transition between the V_o^{+} to V_o^{2+}. The green emission bands are observed at 505 nm, and 538 nm respectively, is ascribed to the interactions between these oxygen and interfacial tin vacancies.

4.2. Effect of SAP-Ally-NCs on the initial and final body weight, weight gain and growth rate of control and experimental rats

Fig. 6 displays the effects of SAP-Ally-NCs on the bodyweight changes of the experimental animals. The DMH-challenged

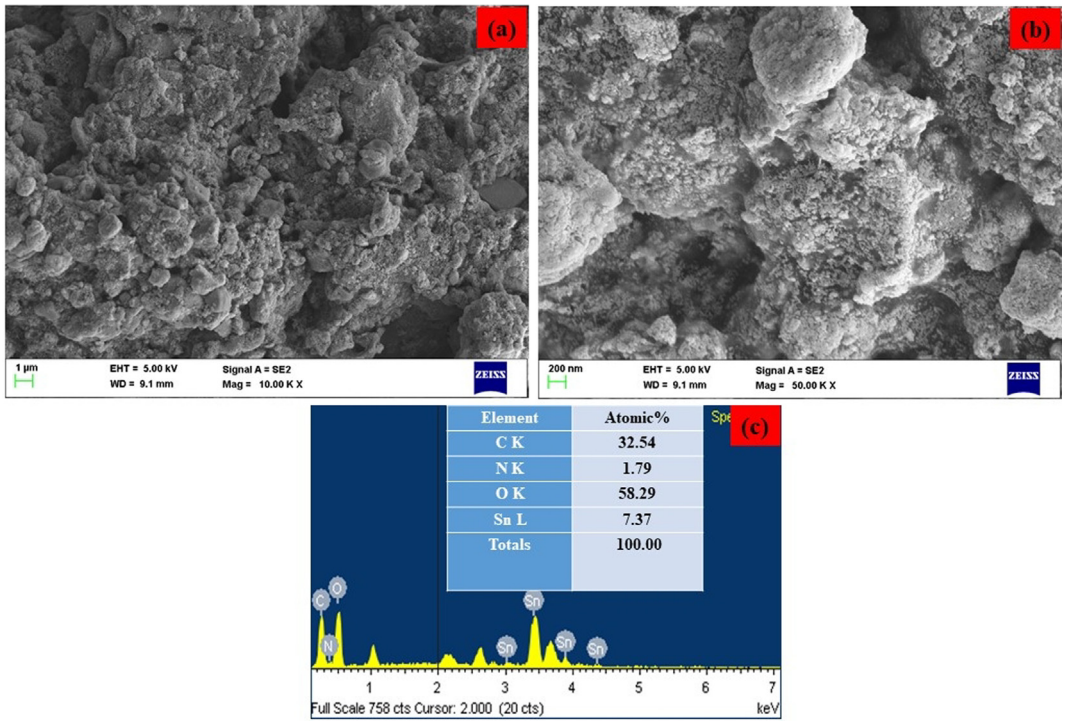

Fig. 2 (a-b). Lower and higher magnification of FE-SEM image and (c) EDX spectrum of SAP- Ally-NCs.

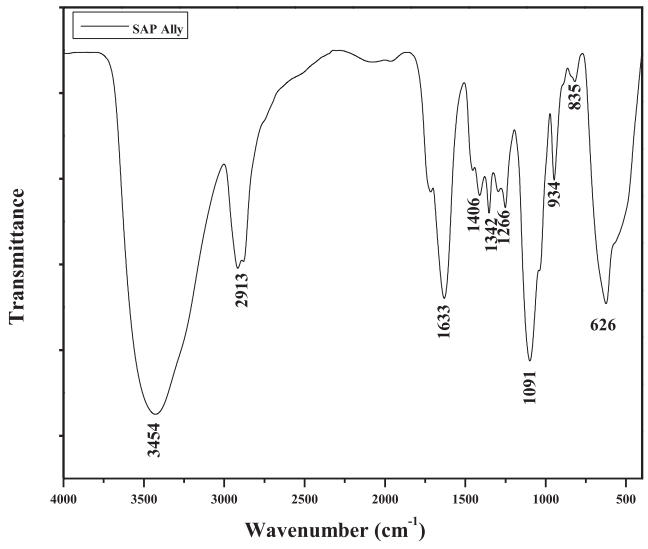

Fig. 3 FT-IR spectrum of SAP- Ally-NCs.

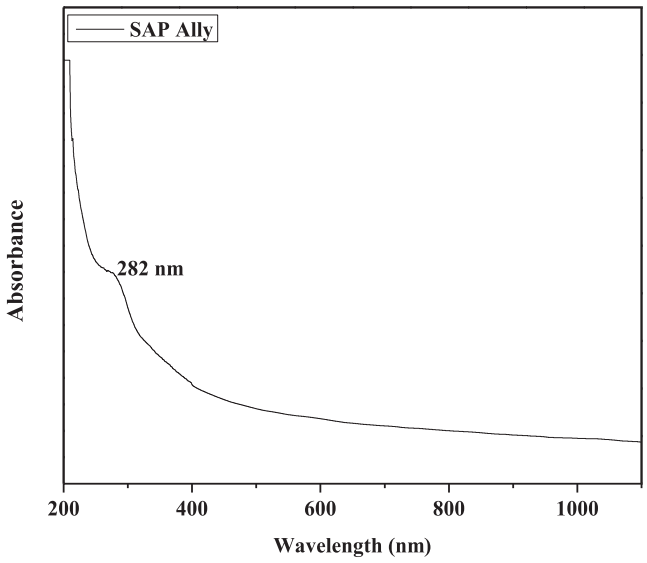

Fig. 4 UV–Vis spectrum of SAP-Ally-NCs.

animals demonstrated a drastic reduction in the final bodyweight, weight gain and growth rate, which is contrasting to the control. On the other hand, the formulated SAP-Ally-NCs supplementation possessed the remarkable bodyweight gain in DMH-activated rats. When compared with the low dose of SAP-Ally-NCs (10 µM/kg) treatment, the high dose of SAP-Ally-NCs (15 µM/kg) was appreciably prevented the weight loss and improved the final bodyweight and growth rate of DMH-triggered animals (Fig. 6). The fabricated SAP-Ally-NCs supplementation effectively regained the bodyweight of animals.

4.3. Effect of SAP-Ally-NCs on the colonic polyps' incidence of experimental rats

As illustrated in the Table 1, the control animals did not possessed any signs of polyps. DMH-activated rats demonstrated the 100% of polyp's incidences, which is in contrast to the control. The formulated SAP-Ally-NCs (10 and 15 µM/kg) supplemented animals displayed a remarkable reduction in the polyp's formation in the DMH-provoked animals (Fig. 7). The supplementation of 10 and 15 µM/kg of formulated SAP-Ally-NCs has effectively prevented the polyp's incidence, respectively.

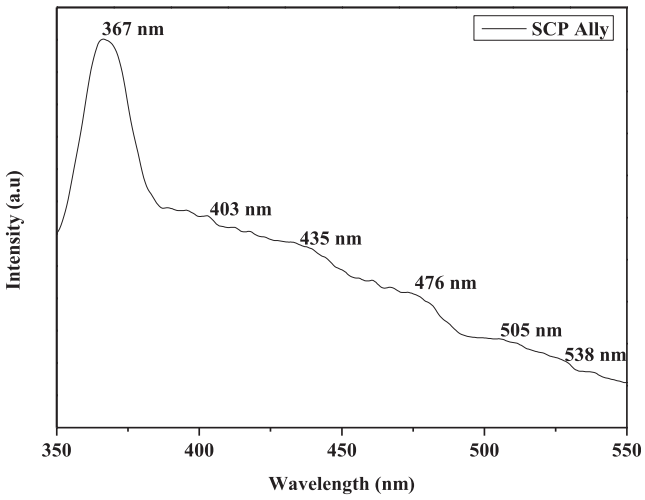

Fig. 5 PL spectrum of SAP-Ally-NCs.

4.4. Effect of SAP-Ally-NCs on the TBARS level in the liver and colon tissues of experimental rats

Fig. 7 demonstrating the TBARS levels of both control and experimental animals. The DMH-provoked animals displayed the augmented status of lipid peroxidation in the liver, proximal and distal colon tissues as evidenced by elevated TBARS status, when compared with control. Interestingly, the supplementation of formulated SAP-Ally-NCs (10 and 15 μM/kg) to the DMH-triggered rats displayed the drastic reduction in the status of TBARS in liver, proximal and distal colon tissues. When compared with low dose, a high dose of SAP-Ally-NCs (15 μM/kg) administration effectively elevated the TBARS status in the DMH-provoked animals.

4.5. Effect of SAP-Ally-NCs on the SOD activity of liver and colon tissues of experimental rats

The liver, proximal, and distal colon tissues of DMH-challenge to the animals demonstrated the severe reduction in the enzy-

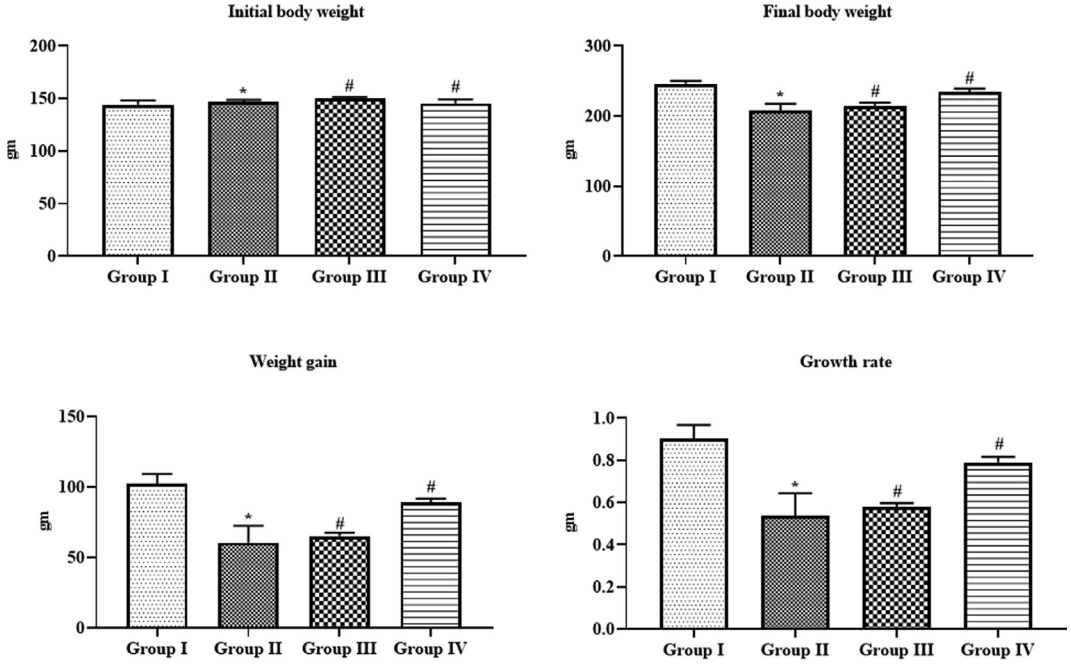

Fig. 6 Effect of SAP-Ally-NCs on the initial and final body weight, weight gain and growth rate of experimental rats, Results were depicted as the mean ± SD from all the discrete groups. One-way ANOVA was applied to illustrate the variations between groups successively Tukey–Kramer's multiple comparison test. Note: '*' $P < 0.05$ compared with control and '#' $P < 0.05$ compared with DMH-provoked group. Group I: control, Group II: 20 mg/kg DMH-challenged animals, Group III & IV: DMH animals supplemented with 10 and 15 μM of SAP-Ally-NCs, respectively.

Table 1 Effect of SAP-Ally-NCs on the colonic polyps' incidence of experimental rats.

Groups	No. of polyp bearing rats	Total number of polyps	Incidence of polyps (%)	Inhibition of polyps (%)	Average numberof polyps/ polyp bearing rat
Group I	Nil	Nil	Nil	–	–
Group II	6	17	100	0	4.12
Group III	4	10	58	42%	3.62
Group IV	2	6	37	65%	2.97

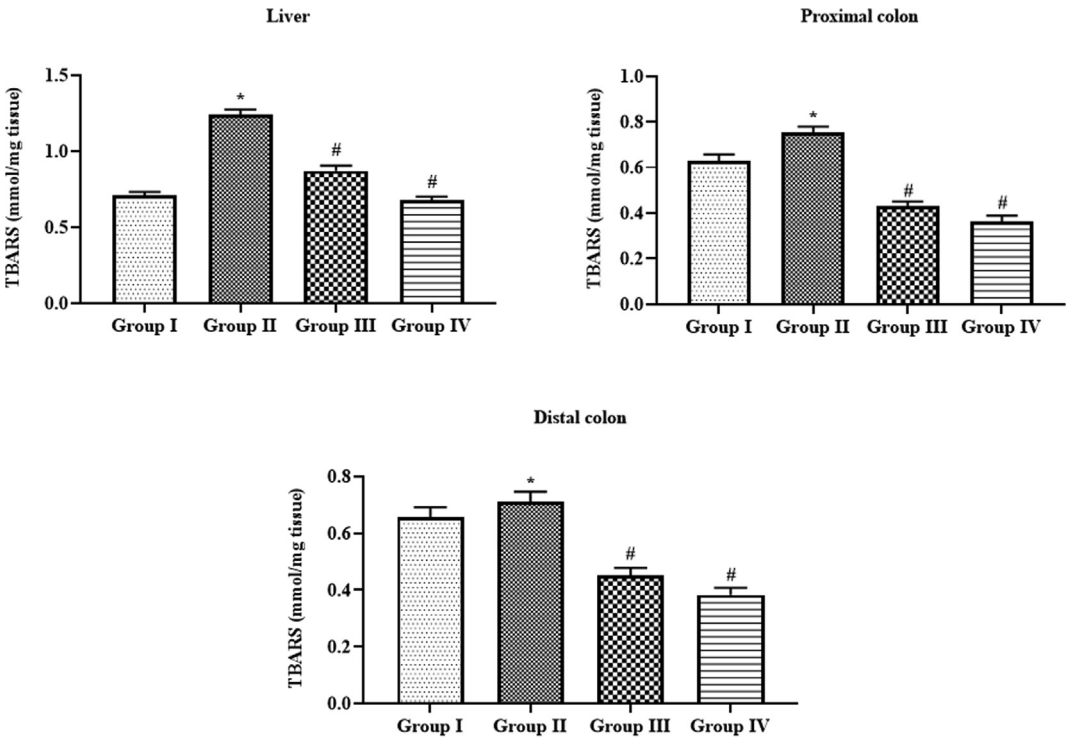

Fig. 7 Effect of SAP-Ally-NCs on the TBARS level in the liver and colon tissues of experimental rats, Results were depicted as the mean ± SD from all the discrete groups. One-way ANOVA was applied to illustrate the variations between groups successively Tukey–Kramer's multiple comparison test. Note: '*' $P < 0.05$ compared with control and '#' $P < 0.05$ compared with DMH-provoked group. Group I: control, Group II: 20 mg/kg DMH-challenged animals, Group III & IV: DMH animals supplemented with 10 and 15 μM of SAP-Ally-NCs, respectively.

matic activity of antioxidant SOD when compared with control (Fig. 8). Surprisingly, the supplementation of 10 and 15 μM/kg of formulated SAP-Ally-NCs were appreciably enhanced the activity of SOD in both liver and colon tissues of DMH-activated animals. The high dose of formulated SAP-Ally-NCs (15 μM/kg) has improved the SOD activity more effectively when compared with low dose treatment.

4.6. Effect of SAP-Ally-NCs on the CAT activity of liver and colon tissues of experimental rats

As illustrated in the Fig. 9, the activity of antioxidant enzyme CAT was diminished drastically in the liver, proximal, and distal colon tissues of DMG-provoked animals. On the other hand, the treatment with the formulated SAP-Ally-NCs were effectively improved the activity of CAT in both liver and colon tissues. When compared with 10 μM/kg, the 15 μM/kg of formulated SAP-Ally-NCs were demonstrated the potent activity, which is evidenced by the increased activity of CAT in the liver and colon tissues. The control and 15 μM/kg of formulated SAP-Ally-NCs administered rats displayed the similar kind of outcomes with each other.

4.7. Effect of SAP-Ally-NCs on the phase I and phase II xenobiotic enzymes in the liver tissues of experimental rats

Fig. 10 revealed that the status of xenobiotic enzymes i.e. cytochrome-P450, cytochrome-B5, cytochrome-p4502E1, and NADPH-cytochrome-P450 reductase in the liver tissues of DMH-activated rats were found up-regulated when compared with control. Interestingly, the administration of formulated SAP-Ally-NCs (10 and 15 μM/kg) were effectively diminished the status of these xenobiotic enzymes and set back to the near normal levels in the liver tissues of DMH-provoked animals. The outcomes of control and 15 μM/kg of formulated SAP-Ally-NCs administered animals were found similar.

4.8. Effect of SAP-Ally-NCs on the inflammatory markers in the serum of experimental rats

The status of TNF-α, IL-6, and IL-1β in the serum of experimental animals was examined and the outcomes were depicted in the Fig. 11. The TNF-α, IL-6, and IL-1β levels were found elevated in the DMH-provoked animals when compared with control. Interestingly, the formulated SAP-Ally-NCs (10 and 15 μM/kg) administration to the DMH-triggered animals were demonstrated the remarkable reduction in the status of TNF-α, IL-6, and IL-1β. The control and 15 μM/kg of formulated SAP-Ally-NCs supplemented animals demonstrated similar kind of outcomes.

4.9. Effect of SAP-Ally-NCs on the mRNA expressions of signaling molecules in the colon tissues of experimental rats

The mRNA expression of various signaling molecules was studied by RT-PCR analysis and the outcomes were depicted

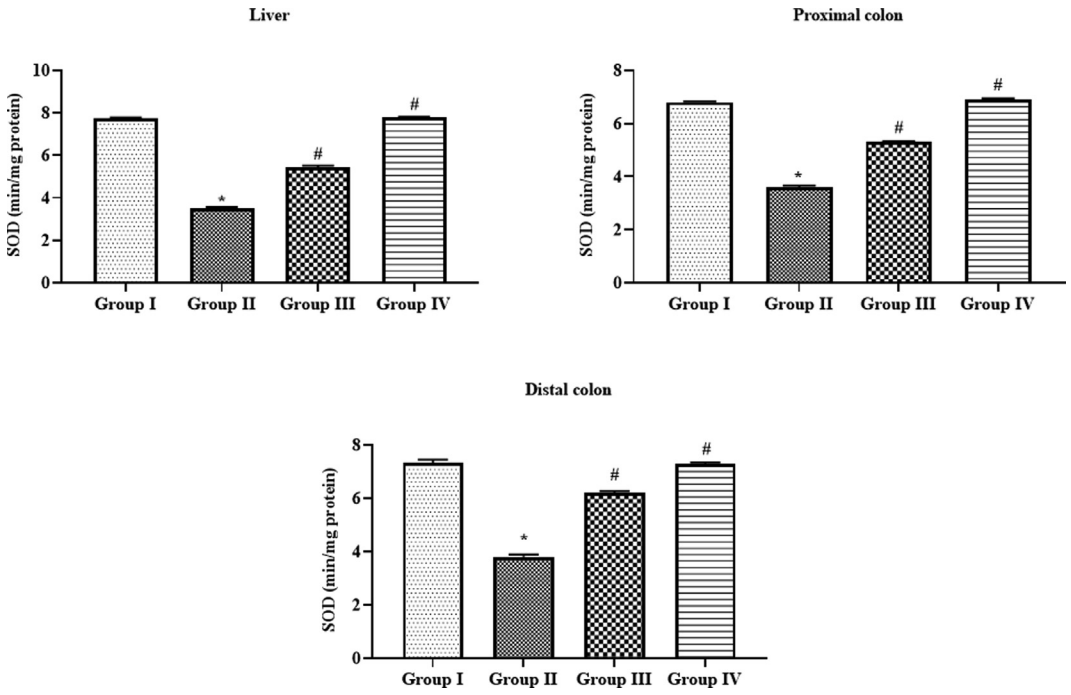

Fig. 8 Effect of SAP-Ally-NCs on the SOD activity in the liver and colon tissues of experimental rats, Results were depicted as the mean ± SD from all the discrete groups. One-way ANOVA was applied to illustrate the variations between groups successively Tukey–Kramer's multiple comparison test. Note: '*' $P < 0.05$ compared with control and '#' $P < 0.05$ compared with DMH-provoked group. Group I: control, Group II: 20 mg/kg DMH-challenged animals, Group III & IV: DMH animals supplemented with 10 and 15 μM of SAP-Ally-NCs, respectively.

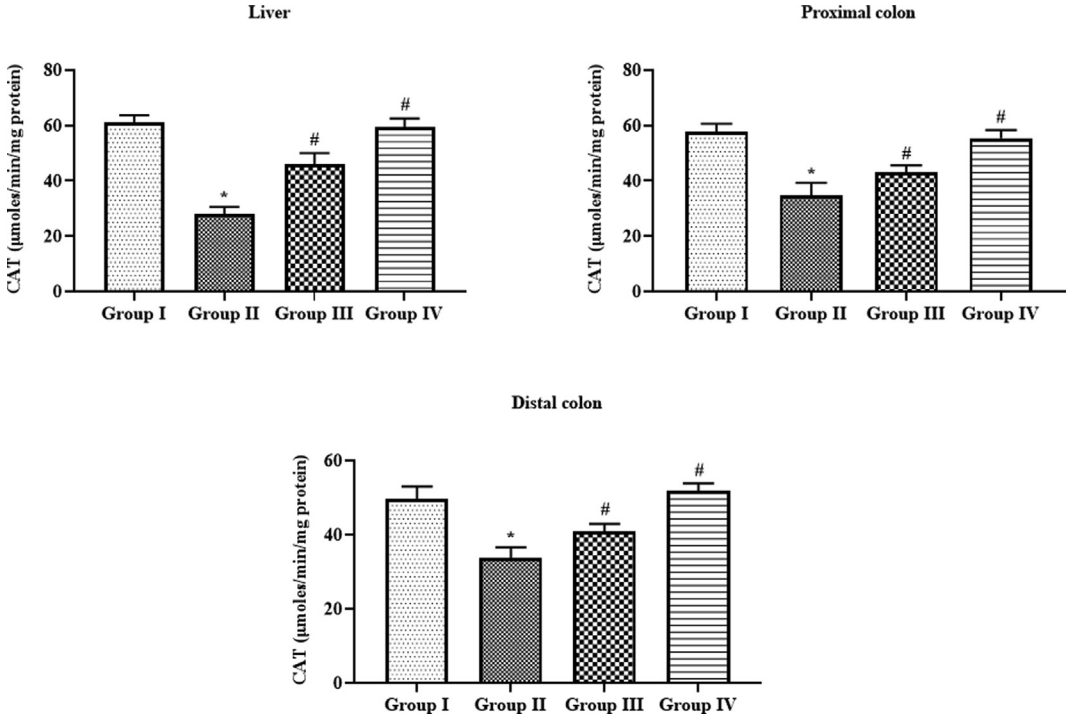

Fig. 9 Effect of SAP-Ally-NCs on the CAT activity in the liver and colon tissues of experimental rats, Results were depicted as the mean ± SD from all the discrete groups. One-way ANOVA was applied to illustrate the variations between groups successively Tukey–Kramer's multiple comparison test. Note: '*' $P < 0.05$ compared with control and '#' $P < 0.05$ compared with DMH-provoked group. Group I: control, Group II: 20 mg/kg DMH-challenged animals, Group III & IV: DMH animals supplemented with 10 and 15 μM of SAP-Ally-NCs, respectively.

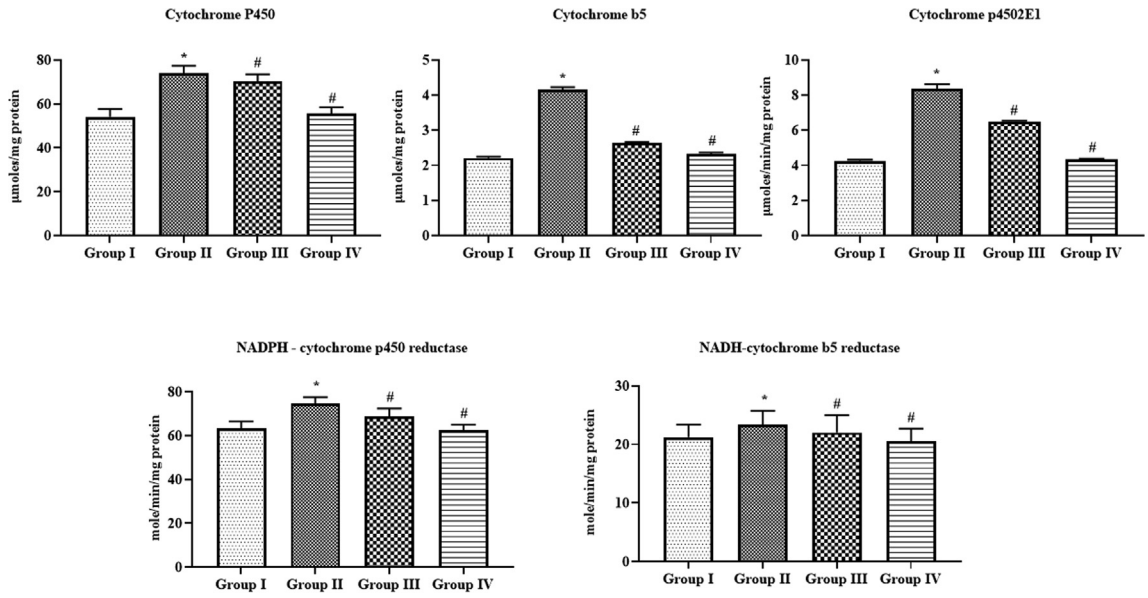

Fig. 10 Effect of SAP-Ally-NCs on the phase I and phase II xenobiotic enzymes in the liver tissues of experimental rats, Results were depicted as the mean ± D from all the discrete groups. One-way ANOVA was applied o illustrate the variations between groups successively Tukey–Kramer's multiple comparison test. Note: '*' $P < 0.05$ compared with control and '#' $P < 0.05$ compared with DMH-provoked group. Group I: control, Group II: 20 mg/kg DMH-challenged animals, Group III & IV: DMH animals supplemented with 10 and 15 µM of SAP-Ally-NCs, respectively.

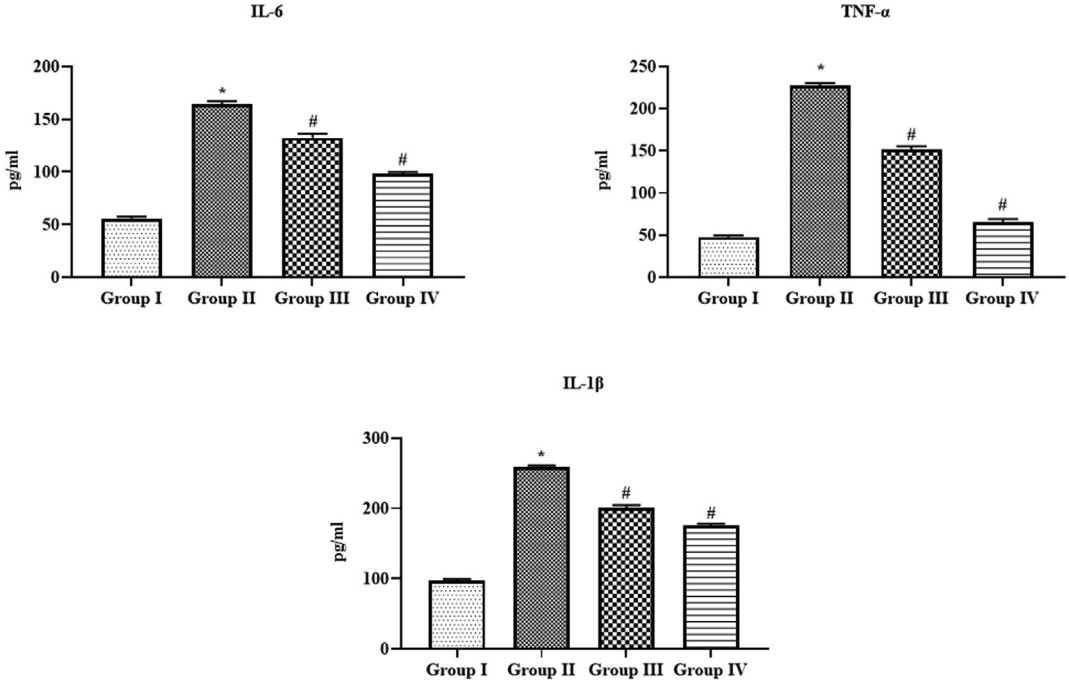

Fig. 11 Effect of SAP-Ally-NCs on the inflammatory markers in the serum of experimental rats. Results were depicted as the mean ± SD from all the discrete groups. One-way ANOVA was applied to illustrate the variations between groups successively Tukey–Kramer's multiple comparison test. Note: '*' $P < 0.05$ compared with control and '#' $P < 0.05$ compared with DMH-provoked group. Group I: control, Group II: 20 mg/kg DMH-challenged animals, Group III & IV: DMH animals supplemented with 10 and 15 µM of SAP-Ally-NCs, respectively.

in the Fig. 12. The mRNA expression of PCNA, cyclin-D1, iNOS, and COX-2 was found up-regulated in the colon tissues of DMH-provoked rats. Surprisingly, the supplementation of formulated SAP-Ally-NCs (10 and 15 µM/kg) was potentially restrained the expression of PCNA, cyclin-D1, iNOS, and COX-2 in the colon tissues of DMH-activated animals.

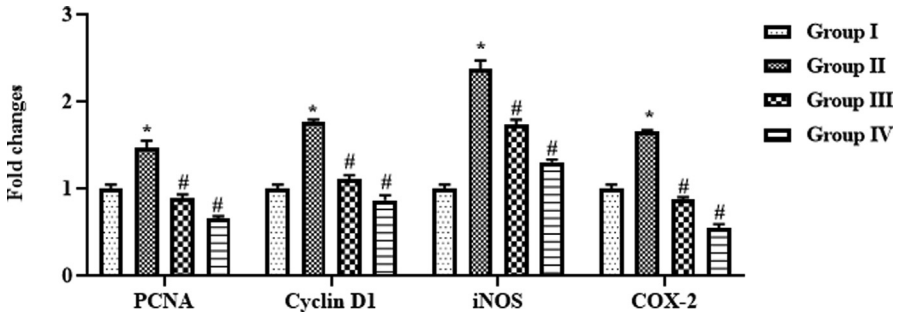

Fig. 12 Effect of SAP-Ally-NCs on the mRNA expressions of signaling molecules in the colon tissues of experimental rats, Results were depicted as the mean ± SD from all the discrete groups. One-way ANOVA was applied to illustrate the variations between groups successively Tukey–Kramer's multiple comparison test. Note: '*' $P < 0.05$ compared with control and '#' $P < 0.05$ compared with DMH-provoked group. Group I: control, Group II: 20 mg/kg DMH-challenged animals, Group III & IV: DMH animals supplemented with 10 and 15 μM of SAP-Ally-NCs, respectively.

4.10. Effect of SAP-Ally-NCs on the colon histology of experimental rats

The histological alterations in the colon tissues of experimental animals were examined by H&E and the microscopic images were displayed in the Fig. 13. Control animals demonstrated the typical cellular arrangements without any lesions. The colon tissues of DMH-triggered animals displayed the severe histological alterations, epithelial lining damages, and glands with dysplasia cells. Interestingly, the treatment with the SAP-Ally-NCs (10 and 15 μM/kg) effectively ameliorated the DMH-activated histological changes and reduced the proliferating cells in the colon tissues of DMH-triggered tissues (Fig. 14).

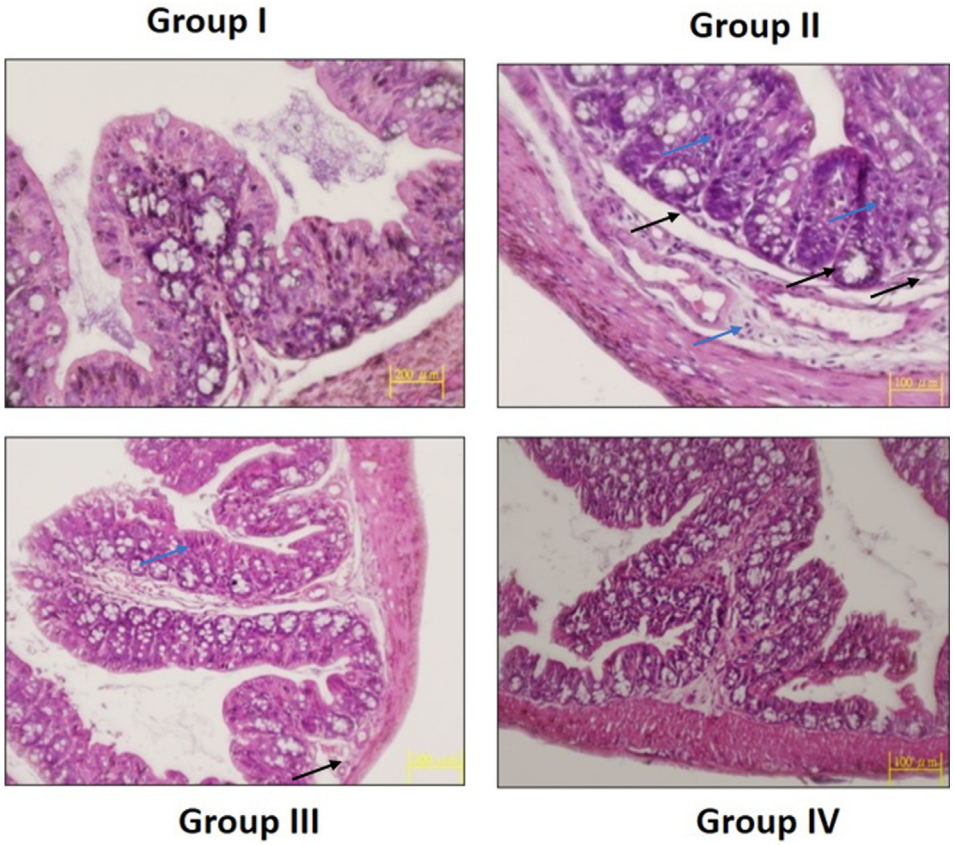

Fig. 13 Effect of SAP-Ally-NCs on the colon histology of experimental rats. Control rats exhibited the usual cellular arrangements without any lesions (Group I). The DMH-triggered animals demonstrated the severe histological alterations, epithelial lining damages (black arrows) with dysplasia (blue arrows) cells (Group II). The SAP-Ally-NCs (10 and 15 μM/kg) treated rats effectively ameliorated the DMH-challenged histological changes (Group III & IV).

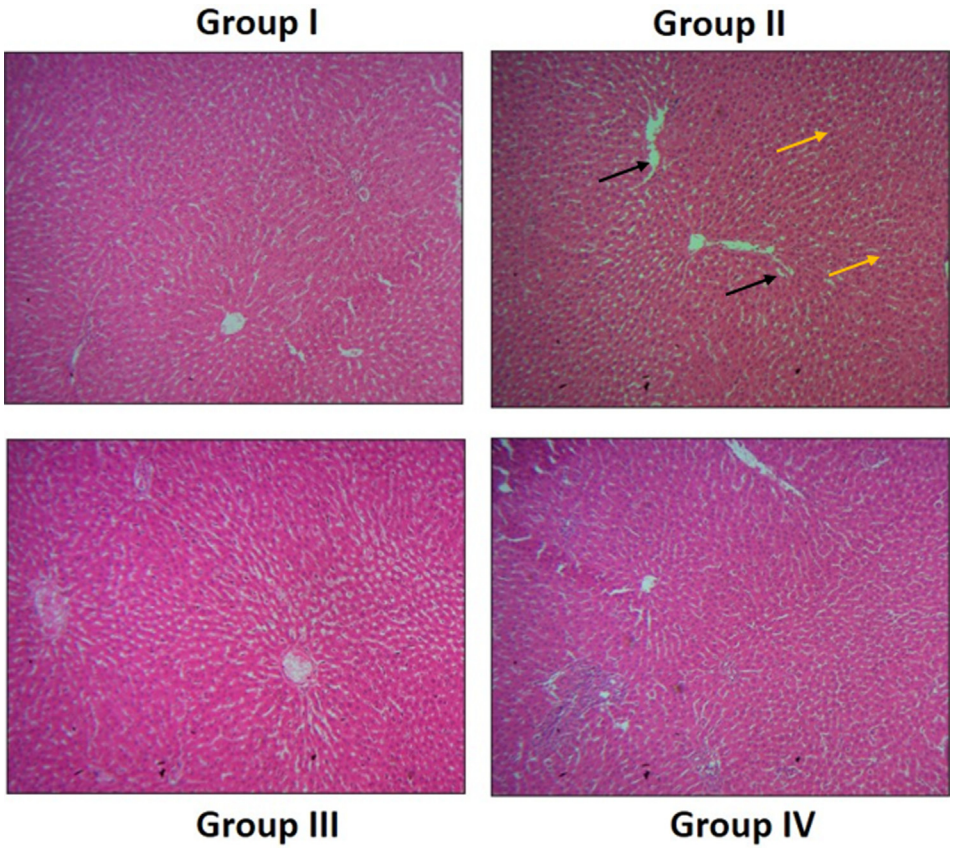

Fig. 14 Effect of SAP-Ally-NCs on the liver histology of experimental rats. The liver tissues of control rats displayed the usual cellular patterns without any damages and lesions (Group I). DMH-challenged rats demonstrated the increased hyperplasia (yellow arrows) and hepatocyte (black arrows) damages (Group II). AP-Ally-NCs (10 and 15 μM/kg) administered animals exhibited the improved liver histology with reduced hepatocytes damages and attenuated the histological changes (Group III & IV).

4.11. Effect of SAP-Ally-NCs on the liver histology of experimental rats

The H&E stained liver tissues of experimental animals were examined microscopically to detect the histological changes and the outcomes were displayed in the Fig. 14. The liver tissues of control rats displayed the usual cellular patterns without any damages and lesions. However, the liver tissues of the DMH-stimulated rats demonstrated the increased hyperplasia, fatty vesicular cells, and injuries in the hepatocytes were found. The SAP-Ally-NCs (10 and 15 μM/kg) administered animals were demonstrated the improved liver histology with reduced hepatocytes damages, which proving the protective effects of formulated SAP-Ally-NCs against DMH-provoked liver damages.

5. Discussion

CRC is a major type of cancer that primarily affects the digestive system and a prime most cause of mortalities globally (Arnold et al., 2020). Characteristics of CRC include unrestrained cell multiplication of colonic crypt epithelial cells, initiating with hyperplasia and gradually developing into aggressive carcinoma (Nabil et al., 2016). DMH-mediated triggering of CRC in animals is recommended as an perfect animal model for crucial investigation of molecular events and participated signaling cascades in the pathological progression of CRC, due to the major similarities of both morphological as well as histologically. DMH is get metabolized into diazonium ion on the liver. This compound is a major reason for the inequality in oxidative stress and DNA damage that could be an initial phase of cancers (Perse and Cerar, 2011).

The progresses in the nanotechnology, such as the development of nanoscale drug delivery, can warrant accurate cancerous tissue targeting with less deleterious effects (Hu et al., 2016; Huang et al., 2019; Hu et al., 2018). In this exploration, we formulated the SAP-Ally-NCs and investigated its anticancer potential against DMH-provoked CRC in rats. The fabricated SAP-Ally-NCs were characterized using different techniques. The SAP-Ally-NCs results of XRD analysis is good agreement with JCPDS no. 88-0287 and peaks show that the tetragonal rutile-type SnO_2 (space group P42/mnm) crystalline structure (Grzeta et al., 2002). FT-IR results revealed that the O-H stretching bands are around 3454 cm^{-1} and 1633 cm^{-1}, correspond to the absorption of water molecules at the sample surface (Moumen et al., 2019). The asymmetric O-Sn-O stretching vibrations have occurred at 835 and 626 cm^{-1}, which has indicated that the SnO_2 (Hussain et al., 2020). The findings from the PL analysis showed the NBE

emission is found to be 367 nm, corresponding to the recombination of electron-hole pairs in oxygen and metal vacancies (Vanheusden et al., 1996). The green emission bands are observed at 505 nm, and 538 nm respectively, is ascribed to the interactions between these oxygen and interfacial tin vacancies (Gu et al., 2003).

Oxidative stress is primarily an outcomes of inequity between free radicals and antioxidant's radical scavenging potential. As stated earlier, liver is the detrimental site of DMH activation that leads to over accumulation of ROS. As well, augmented oxidative stress in the liver may imitate alterations in the intestinal regions (Brenner et al., 2015). In particular, a continual inflammation/environmental factors lead to an elevated oxidative stress in a CRC progression, which must be repressed in the precancerous phase as a response of anticancer therapy (Takaki et al., 2019). In this study, we found the augmented TBARS with diminished antioxidants status in the liver and colon tissues of DMH-challenged animals. Substantially, the administration of the formulated SAP-Ally-NCs appreciably declined the TBARS and improved the activity of SOD and CAT in both liver and colon tissues. This outcome evidenced the antioxidant potential of formulated SAP-Ally-NCs.

The uninterrupted accumulation of pro-inflammatory regulators like IL-6, IL-1β, and TNF-α was tightly connected with the human CRC (Akhmaltdinova et al., 2020). TNF-α is an imperative pro-inflammatory marker that numerous studies has demonstrated that its expression was up-regulated in CRC. The expression of TNF-α is directly dependent on the stimulation of NF-κB that is one of the prime inflammatory regulator. Hence, targeting of TNF-α could be an effective strategy to treat the CRC (Hirano et al., 2020). Similarly, we also noted that enhanced status of IL-6, IL-1β, and TNF-α in the DMH-provoked animals. Surprisingly, the SAP-Ally-NCs treatment effectively diminished the IL-6, IL-1β, and TNF-α status in the serum of DMH-challenged animals. This outcome evidenced the anti-inflammatory potential of SAP-Ally-NCs.

Inflammation and oxidative stress contributes an immense role and are accounted to instigation and progression of various tumors (Bickers and Athar, 2006). COX-2, an imperative indicator of inflammation is stimulated during inflammatory response and its expressions were enhanced in adenomas and it was documented that it over-expressed in CRC (Eberhart et al., 1994; Sano et al., 1995). COX- 2 was well-known to perform a vital function in the colon toxicity and the development of polyp. Consequently, its inhibition has said to be a trustworthy approach of chemotherapeutic strategy of CRC and other colon associated ailments (Taketo, 1998). COX-2 is activated in hypoxic/inflammatory situations and is up-regulated in numerous cancers, including CRC, contrasting in normal cells, which makes it as a reliable therapeutic target (Liu et al., 2015). It is already demonstrated that elevated expression of (iNOS) and COX-2 is closely connected with the CRC (Umesalma and Sudhandiran, 2010). Excessive COX-2 expression was monitored in numerous pre-malignant and malignant conditions (Williams et al., 1999; Mohan and Epstein, 2003). It was found that COX-2 is triggered promptly in response to numerous growth factors and inflammatory cytokines (Aggarwal and Gehlot, 2009). It was also found that the iNOS has the central functions in the colon toxicity (Eizirik and Pavlovic, 1997). The over generation of nitric oxide (NO) via iNOS could provoke the DNA injury via diverse mechanisms. It is also participated in the diverse pathological as well as physiological situations and contributes an essential function in the tumor progression (Hofseth, 2008).

Femia et al. (2010) suggested that the DMH-provoked CRC has the greater expression of pro-inflammatory enzyme iNOS. PCNA, a supportive protein to DNA polymerase is a co-factor of synthesis of DNA and its expression in elevated in the proliferating cells (Fairman, 1990). Thereby, detection of PCNA expressions was regarded as a most trustworthy approach to investigate the proliferation status of colon tissues (Biasco et al., 1994). DMH-provoked rats demonstrated the up-regulated mRNA expressions of PCNA, cyclin-D1, iNOS, and COX-2 in the colon tissues. But the SAP-Ally-NCs treatment appreciably repressed the PCNA, cyclin-D1, iNOS, and COX-2 expressions in the DMH-activated animals. This outcome proved that the SAP-Ally-NCs could inhibit the cell proliferative and inflammatory signaling pathways in the DMH-triggered CRC animals.

CRC development is a multifaceted event with dysregulation of mucosal epithelial cells and irregular cell multiplications. The preceding reports on CRC models are categorized by assorted microscopically detectable mucosal intraepithelial lesions. Histologically, these lesions demonstrate various characteristics ranging from slight hyperplasia to deleterious dysplasia (Jass, 2002). In accordance with this statement, we also found the drastic histological alterations in both colon and liver tissues of DMH-challenged rats and these alterations were appreciably ameliorated by the SAP-Ally-NCs treatment.

6. Conclusion

In conclusion, the formulated SAP-Ally-NCs have displayed the potent anticancer action against the DMH-provoked CRC in rats. The SAP-Ally-NCs administration effectively improved the body-weight gain and declined the polyp's incidences. SAP-Ally-NCs also decreased the inflammatory markers and oxidative stress and improved the antioxidants SOD and CAT in both liver and colon tissues of DMH-challenged animals. SAP-Ally-NCs treatment appreciably down-regulated the mRNA expressions of PCNA, cyclin-D1, iNOS, and COX-2 in the colon tissues. The histological findings also demonstrated the therapeutic role of formulated SAP-Ally-NCs against the DMH-provoked CRC in animals. In future, SAP-Ally-NCs could be a potent chemotherapeutic agent to the CRC.

Declaration of Competing Interest

The authors declare that they have no known competing financial interests or personal relationships that could have appeared to influence the work reported in this paper.

References

Aebi, H., 1984. Catalase in vitro. In: Methods in Enzymology, vol. 105. Academic Press: Cambridge, MA, USA, pp. 121–126.

Aggarwal, B.B., Gehlot, P., 2009. Inflammation and cancer: how friendly is the relationship for cancer patients?. Curr. Opin. Pharmacol. 9, 351–369.

Ahmed, K., Zaidi, S.F., Cui, Z., Zhou, D., Saeed, S.A., Inadera, H., 2019. Potential proapoptotic phytochemical agents for the treatment and prevention of colorectal cancer. Oncol. Lett. 18, 487–498.

Akhmaltdinova, L., Sirota, V., Babenko, D., Zhumaliyeva, V., Kadyrova, I., Maratkyzy, M., Ibrayeva, A., Avdienko, O., 2020.

Proinflammatory cytokines and colorectal cancer-the impact of the stage. Contemp Oncol (Pozn). 24 (4), 207–210.
Arnold, M., Abnet, C.C., Neale, R.E., Vignat, J., Giovannucci, E.L., McGlynn, K.A., Bray, F.J.G., 2020. Global burden of 5 major types of gastrointestinal cancer. Gastroenterology 159, 335–349.
Biasco, G., Paganelli, G.M., Santucci, R., Brandi, G., Barbara, L., 1994. Methodological problems in the use of rectal cell proliferation as a biomarker of colorectal cancer risk. J. Cell Biochem. 19, 55–60.
Bickers, D.R., Athar, M., 2006. Oxidative stress in the pathogenesis of skin disease. J. Invest. Dermatol. 126, 2565–2575.
Birben, E., Sahiner, U.M., Sackesen, C., Erzurum, S., Kalayci, O., 2012. Oxidative stress and antioxidant defense. World Allergy Organ. J. 5 (1), 9.
Braun, M.S., Seymour, M.T., 2011. Balancing the efficacy and toxicity of chemotherapy in colorectal cancer. Ther. Adv. Med. Oncol. 3, 43–52.
Bray, F., Ferlay, J., Soerjomataram, I., Siegel, R.L., Torre, L.A., Jemal, A., 2018. Global cancer statistics 2018: GLOBOCAN estimates of incidence and mortality worldwide for 36 cancers in 185 countries. CA Cancer J. Clin. 68, 394–424.
Brenner, D.A., Paik, Y.-H., Schnabl, B., 2015. Role of Gut Microbiota in Liver Disease. J. Clin. Gastroenterol. 49, S25–S27.
Cai, F., Li, J., Pan, X., Zhang, C., Wei, D., Gao, C., 2017. Increased Expression of PCNA-AS1 in Colorectal Cancer and its Clinical Association. Clin. Lab. 63, 1809–1814.
Colussi, C., Fiumicino, S., Giuliani, A., Rosini, S., Musiani, P., Macrí, C., Potten, C.S., Crescenzi, M., Bignami, M.J., 2001. 1, 2-dimethylhydrazine-induced colon carcinoma and lymphoma in msh2(-/-) mice. J Natl Cancer Inst. 93, 1534–1540.
De Almeida, C.V., de Camargo, M.R., Russo, E., Amedei, A., 2018. Role of diet and gut microbiota on colorectal cancer immunomodulation. World J. Gastroenterol. 25, 151–162.
Eberhart, C.E., Coffey, R.J., Radhika, A., Giardiello, F.M., Ferrenbach, S., DuBois, R.N., 1994. Up-regulation of cyclooxygenase 2 gene expression in human colorectal adenomas and adenocarcinomas. Gastroenterology 107, 1183–1188.
Eizirik, D.L., Pavlovic, D., 1997. Is there a role for nitric oxide in beta-cell dysfunction and damage in IDDM?. Diab. Metab. Rev. 13, 293–307.
Fairman, M.P., 1990. DNA polymerase delta/PCNA: actions and interactions. J. Cell Sci. 95, 1–4.
Femia, A.P., Luceri, C., Toti, S., Giannini, A., Dolara, P., Caderni, G., 2010. Gene expression profile and genomic alterations in colonic tumours induced by 1,2-dimethylhydrazine (DMH) in rats. BMC Cancer 10, 194.
Gan, L., von Moltke, L.L., Trepanier, L.A., Harmatz, J.S., Greenblatt, D.J., 2009 Jan 1. Role of NADPH-cytochrome P450 reductase and cytochrome-b5/NADH-b5 reductase in variability of CYP3A activity in human liver microsomes. Drug Metab. Dispos. 37 (1), 90–96.
Grzeta, B., Tkalcec, E., Goebbert, C., Takeda, M., Takahashi, M., Nomura, K., Jaksic, M., 2002. Structural studies of nanocrystalline SnO_2 doped with antimony: XRD and Mossbauer spectroscopy. J. Phys. Chem. Solids 63 (5), 765–772.
Gu, F., Wang, S.F., Song, C.F., Lü, M.K., Qi, Y.X., Zhou, G.J., Yuan, D.R., 2003. Synthesis and luminescence properties of SnO_2 nanoparticles. Chem. Phys. Lett. 372 (3–4), 451–454.
Guimaraes, P.P.G., Oliveira, S.R., de Castro Rodrigues, G., Gontijo, S.M.L., Lula, I.S., Cortés, M.E., Denadai, Â.M.L., Sinisterra, R.D. J.M., 2015. Development of sulfadiazine-decorated plga nanoparticles loaded with 5-fluorouracil and cell viability. Molecules 20, 879–899.
Gullotti, E., Yeo, Y., 2009. Extracellularly activated nanocarriers: A new paradigm of tumor targeted drug delivery. Mol. Pharm. 6, 1041–1051.
Guzinska-Ustymowicz, K., Pryczynicz, A., Kemona, A., Czyzewska, J., 2009. Correlation between proliferation markers: PCNA, Ki-67, MCM-2 and antiapoptotic protein Bcl-2 in colorectal cancer. Anticancer Res. 29, 3049–3052.
Hammond, W.A., Swaika, A., Mody, K., 2016. Pharmacologic resistance in colorectal cancer: A review. Ther. Adv. Med. Oncol. 8, 57–84.
Hirano, T., Hirayama, D., Wagatsuma, K., Yamakawa, T., Yokoyama, Y., Nakase, H., 2020. Immunological mechanisms in inflammation-associated colon carcinogenesis. Int. J. Mol. Sci. 21 (9), 3062.
Hofseth, L.J., 2008. Nitric oxide as a target of complementary and alternative medicines to prevent and treat inflammation and cancer. Cancer Lett 268, 10–30.
Hu, J., Huang, S., Zhu, L., Huang, W., Zhao, Y., Jin, K., ZhuGe, Q., 2018. Tissue Plasminogen Activator-Porous Magnetic Microrods for Targeted Thrombolytic Therapy after Ischemic Stroke. ACS Appl Mater Interfaces. 10, 32988–32997.
Hu, J., Huang, W., Huang, S., ZhuGe, Q., Jin, K., Zhao, Y., 2016. Magnetically active Fe3O4 nanorods loaded with tissue plasminogen activator for enhanced thrombolysis. NANO Research. 9, 2652–2661.
Huang, D., Wu, K., Zhang, Y., Ni, Z., Zhu, X., Zhu, C., Jianjing, Y., Qichuan, Z., Jiangnan, H., 2019. Recent Advances in Tissue plasminogen activator-based nanothrombolysis for ischemic stroke. Review Adv Material Sci. 58 (1), 159–170.
Hussain, N., Zulfiqar, S., Khan, T., Khan, R., Khattak, S.A., Ali, S., Khan, G., 2020. Investigation of structural, optical, dielectric and magnetic properties of Sno_2 nanorods and nanospheres. Mater. Chem. Phys. 241, 122382.
Hwang, E.S., Lee, H.J., 2006. Allyl isothiocyanate and its N-acetylcysteine conjugate suppress metastasis via inhibition of invasion, migration, and matrix metalloproteinase-2/-9 activities in SKHep 1 human hepatoma cells. Exp Biol Med 231, 421e30.
Ionov, Y., Peinado, M.A., Malkhosyan, S., Shibata, D., Perucho, M., 1993. Ubiquitous somatic mutations in simple repeated sequences reveal a new mechanism for colonic carcinogenesis. Nature 363, 558–561.
Jass, J.R., 2002. Pathogenesis of colorectal cancer. Surg. Clin. N. Am. 82, 891–904.
Klampfer, L., 2011. Cytokines, inflammation and colon cancer. Curr. Cancer Drug Targets 11, 451–464.
Liu, B., Qu, L., Yan, S., 2015. Cyclooxygenase-2 promotes tumor growth and suppresses tumor immunity. Cancer Cell Int. 15, 106.
Liu, H., Liu, X., Zhang, C., Zhu, H., Xu, Q., Bu, Y., Lei, Y., 2017. Redox Imbalance in the Development of Colorectal Cancer. J. Cancer 8, 1586–1597.
Mariani, F., Sena, P., Roncucci, L., 2014. Inflammatory pathways in the early steps of colorectal cancer development. World J. Gastroenterol. 20, 9716–9731.
Marklund, S.L., 1985. Product of extracellular-superoxide dismutase catalysis. FEBS Lett. 184, 237–239.
Mohan, S., Epstein, J.B., 2003. Carcinogenesis and cyclooxygenase: the potential role of COX-2 inhibition in upper aerodigestive tract cancer. Oral Oncol 39, 537–546.
Mohanty, A., Uthaman, S., Park, I.K., 2020. Utilization of polymer-lipid hybrid nanoparticles for targeted anti-cancer therapy. Molecules 25, 4377.
Moumen, A., Hartiti, B., Comini, E., Arachchige, H.M.M., Fadili, S., Thevenin, P., 2019. Preparation and characterization of nanostructured CuO thin films using spray pyrolysis technique. Superlattices and Microstructures 127, 2–10.
Mukherjee, A., Waters, A.K., Kalyan, P., Achrol, A.S., Kesari, S., Yenugonda, V.M., 1937. Lipid–polymer hybrid nanoparticles as a next-generation drug delivery platform: State of the art, emerging technologies, and perspectives. Int. J. Nanomed. 2019, 14.
Nabil, H.M., Hassan, B.N., Tohamy, A.A., Waaer, H.F., Moneim, A. E.A., 2016. Radioprotection of 1,2-dimethylhydrazine-initiated colon cancer in rats using low-dose γ rays by modulating multidrug

resistance-1, cytokeratin 20, and β-catenin expression. Hum Exp Toxicol. 35 (3), 282–292.
Naik, K., Chandran, V.G., Rajashekaran, R., Waigaonkar, S., Kowshik, M., 2016. Mechanical properties, biological behaviour and drug release capability of nano TiO2-HAp-Alginate composite scaffolds for potential application as bone implant material. J. Biomater. Appl. 31, 387–399.
Newell, L.E., Heddle, J.A., 2004. The potent colon carcinogen, 1,2-dimethylhydrazine induces mutations primarily in the colon. Mutat Res 564, 1–7.
Ohkawa, H., Ohishi, N., Yagi, K., 1979. Assay for lipid peroxides in animal tissue by thiobarbituric acid reaction. Anal Biochem 95, 351–358.
Omura, T., Sato, R., 1964. The carbon monoxide binding pigment of the liver microsomes. i. evidence for its hemoprotein nature. J Biol Chem 239, 2370–2378.
Perse, M., Cerar, A., 2011. Morphological and Molecular Alterations in 1,2 Dimethylhydrazine and Azoxymethane Induced Colon Carcinogenesis in Rats. J. Biomed. Biotechnol. 2011, 473964.
Pisoschi, A.M., Pop, A., 2015. The role of antioxidants in the chemistry of oxidative stress: A review. Eur. J. Med. Chem. 97, 55–74.
Poti, J.M., Braga, B., Qin, B., 2017. Ultra-processed Food Intake andObesity: What ReallyMatters for Health—Processing or Nutrient Content?. Curr. Obes. Rep. 6, 420–431.
Qin, G., Li, P., Xue, Z., 2018. Effect of allyl isothiocyanate on the viability and apoptosis of the human cervical cancer HeLa cell line in vitro. Oncol Lett 15, 8756e60.
Rashid, S., 2017. Cancer and Chemoprevention: An Overview, Springer Science and Business Media LLC, Berlin/Heidelberg, Germany, pp. 173.
Saini, M.K., Sharma, P., Kaur, J., Sanyal, S.N., 2009. The cyclooxygenase-2 inhibitor etoricoxib is a potent chemopreventive agent of colon carcinogenesis in the rat model. J. Environ. Pathol. Toxicol. Oncol. 28, 39–46.
Sano, H., Kawahito, Y., Wilder, R.L., et al, 1995. Expression of cyclooxygenase-1 and -2 in human colorectal cancer. Cancer Res. 55, 3785–3789.
Savio, A.L., da Silva, G.N., Salvadori, D.M., 2015. Inhibition of bladder cancer cell proliferation by allyl isothiocyanate (mustard essential oil). Mutat. Res. 771, 29e35.
Schieber, M., Chandel, N.S., 2014. ROS function in redox signaling and oxidative stress. Curr. Biol. 24 (10), R453–R462.
Senedese, J.M., Rinaldi-Neto, F., Furtado, R.A., Nicollela, H.D., De Souza, L.D.R., Ribeiro, A.B., Ferreira, L.S., Magalhães, G.M., Carlos, I.Z., Da Silva, J.J.M., Tavares, D.C., Bastos, J.K., 2019. Chemopreventive role of Copaifera reticulata Ducke oleoresin in colon carcinogenesis. Biomed. Pharmacother. 111, 331–337.
Sharma, H.K., Ingle, S., Singh, C., Sarkar, B.C., Upadhyay, A., 2012. Effect ofvarious process treatment conditions on the allyl isothiocyanate extraction rate from mustard meal. J. Food Sci. Technol. 49, 368–372.
Sosa, V., Moliné, T., Somoza, R., Paciucci, R., Kondoh, H., LLeonart, M.E., 2013. Oxidative stress and cancer: an overview. Ageing Res. Rev. 12 (1), 376–390.
Takaki, A., Kawano, S., Uchida, D., Takahara, M., Hiraoka, S., Okada, H., 2019. Paradoxical Roles of Oxidative Stress Response in the Digestive System before and after Carcinogenesis. Cancers 11, 213.
Taketo, M.M., 1998. COX-2 and colon cancer. Inflamm Res 47, 112–116.
Tang, S., Wang, Z., Li, P., Li, W., Li, C., Wang, Y., Chu, P.K., 2018. Degradable and photocatalytic antibacterial Au-TiO2/sodium alginate nanocomposite films for active food packaging. Nanomaterials 8 (11), 930.
Thakur, S., Arotiba, O., 2018. Synthesis, characterization and adsorption studies of an acrylic acid-grafted sodium alginate-based TiO2 hydrogel nanocomposite. Adsorpt. Sci. Technol. 36, 458–477.
Tripathi, K., Hussein, U.K., Anupalli, R., Barnett, R., Bachaboina, L., Scalici, J., Rocconi, R.P., Owen, L.B., Piazza, G.A., Palle, K., 2015. Allyl isothiocyanate induces replicationassociated DNA damage response in NSCLC cells and sensitizes to ionizing radiation. Oncotarget 6, 5237e52.
Tuomisto, A.E., Mäkinen, M.J., Väyrynen, J.P., 2019. Systemic inflammation in colorectal cancer: Underlying factors, effects, and prognostic significance. World J. Gastroenterol. 25, 4383–4404.
Umesalma, S., Sudhandiran, G., 2010. Differential inhibitory effects of the polyphenol ellagic acid on inflammatory mediators NF-kB, iNOS, COX-2, TNF-a, and IL-6 in 1,2-dimethylhydrazine-induced rat colon carcinogenesis. J Compilation Nordic Pharmacological Society. Basic Clin. Pharmacol. Toxicol. 107, 650–665.
Van Cutsem, E., Cervantes, A., Adam, R., Sobrero, A., Van Krieken, J.H., Aderka, D., Aranda Aguilar, E., Bardelli, A., Benson, A., Bodoky, G., et al, 2016. ESMO consensus guidelines for the management of patients with metastatic colorectal cancer. Ann. Oncol. 27, 1386–1422.
Van der Stok, E.P., Spaander, M.C.W., Grunhagen, D.J., Verhoef, C., Kuipers, E.J., 2017. Surveillance after curative treatment for colorectal cancer. Nat. Rev. Clin. Oncol. 14, 297–315.
Vanheusden, K., Warren, W.L., Seager, C.H., Tallant, D.R., Voigt, J. A., Gnade, B.E., 1996. Mechanisms behind green photoluminescence in ZnO phosphor powders. J. Appl. Phys. 79 (10), 7983–7990.
Watt, K.C., Plopper, C.G., Buckpitt, A.R., 1997. Measurement of cytochrome P4502E1 activity in rat tracheobronchial airways using high-performance liquid chromatography withelectrochemical detection. Anal Biochem. 248, 26–30.
Williams, C.S., Mann, M., DuBois, R.N., 1999. The role of cyclooxygenases in inflammation, cancer, and development. Oncogene 18, 7908–7916.
Wu, B., Lu, S.-T., Zhang, L.-J., Zhuo, R.-X., Xu, H.-B., Huang, S., 1853. Codelivery of doxorubicin and triptolide with reductionsensitive lipid–polymer hybrid nanoparticles for in vitro and in vivo synergistic cancer treatment. Int. J. Nanomed. 2017, 12.
Zhang, Y., 2010. Allyl isothiocyanate as a cancer chemopreventive phytochemical. Mol Nutr Food Res 54, 127e35.
Zhou, J., Zhang, K., Ma, S., Liu, T., Yao, M., Li, J., Wang, X., Guan, F., 2019. Preparing an injectable hydrogel with sodium alginate and Type I collagen to create better MSCs growth microenvironment. E-Polymers 19, 87–91.